SLAC-PUB-7995
PPRC-TN-98-6
November 1998

Spin-Polarized Electron Emission from Superlattices with Zero Conduction Band Offset*

A. V. Subashiev[1], Yu. A. Mamaev[1], Yu. P. Yashin[1], A. N. Ambrazhei[1],
J. E. Clendenin[2], T. Maruyama[2], G. A. Mulhollan[2],
A. Yu. Egorov[3], V. M. Ustinov[3], A. E. Zhukov[3]

(1) St. Petersburg Technical University, St. Petersburg, 195251, Russia
(2) Stanford Linear Accelerator Center, Stanford, CA 94309, USA
(3) Ioffe Physico-Technical Institute, RAS, St. Petersburg, 194021, Russia

Abstract

Electron spin polarization as high as 86% has been reproducibly obtained from strained $Al_xIn_yGa_{1-x-y}As/GaAs$ superlattice with minimal conduction band offset at the heterointerfaces. The modulation doping of the SL provides high polarization and high quantum yield at the polarization maximum. The position of the maximum can be easily tuned to an excitation wavelength by choice of the SL composition. Further improvement of the emitter parameters can be expected with additional optimization of the SL structure parameters.

Presented at the
Low Energy Polarized Electron Workshop
St. Petersburg, Russia
September 2-5, 1998

* Work supported by Department of Energy contract DE-AC03-76SF00515.

Spin-Polarized Electron Emission from Superlattices with Zero Conduction Band Offset.

A. V. Subashiev[1], Yu. A. Mamaev[1], Yu. P. Yashin[1], A. N. Ambrazhei[1],
J. E. Clendenin[2], T. Maruyama[2], G. A. Mulhollan[2],
A. Yu. Egorov[3], V. M. Ustinov[3], A. E. Zhukov[3]

(1) St. Petersburg Technical University, St. Petersburg, 195251, Russia
(2) Stanford Linear Accelerator Center, Stanford, CA 94309, USA
(3) Ioffe Physico-Technical Institute, RAS, St. Petersburg, 194021, Russia

The development of new sources of highly polarized electrons is motivated by their successful and growing applications in high energy physics, atomic physics, studies of thin films, and surface magnetism. A major breakthrough in achieving an electron polarization of >50% was made in early 1991 with a strained InGaAs on GaAs buffer substrate and GaAs on GaAsP structures [1]. The strain-induced valence-band splitting results potentially in 100% electronic optical orientation under excitation by circularly polarized light at the interband absorption edge. Electron transport to the surface followed by emission into vacuum is accompanied by spin relaxation and thus by polarization losses in the range of 10-20%, consistent with the observed values of polarization of emitted electrons. Emission of polarized electrons into vacuum is provided by activation of the clean GaAs surface by using Cs oxide deposition which reduces the electron work function and leads to band bending at the surface and subsequently a negative electron affinity (NEA) surface.

Polarized electron sources (PES) having significantly higher polarization and electron beam intensity would have an enormous impact on the physics capabilities of future electron-positron colliders and of surface studies installations [2-4]. Further improvements of the GaAs strained layer cathodes are limited by the controversial character of the demands on the cathode heterostructure parameters. High polarization requires high stress in the GaAs layer. Highly stressed layers have small critical-layer thicknesses beyond which the strain gradually relaxes due to structural defects. On the other hand, the active layer thickness should be much thicker than the width of the band bending region. Therefore a thickness close to 100nm is found to be optimal.

Besides the polarization, the electron charge that can be extracted is an essential parameter of a photocathode since it has been found that there is a limit to current density that can be extracted from a GaAs film [5]. To have both higher yield and charge, high doping (up to 5×10^{19}cm^{-3}) of the GaAs layer is needed. High doping reduces the spin relaxation time and thus the electron polarization. Suppressing both polarization losses and charge limit effects is possible by modulation doping with high concentration only in the final 5-7nm surface layer [6].

An alternative source of highly polarized electrons is a semiconductor superlattice (SL) in which the valence band splitting is a consequence of hole confinement in the SL quantum wells (QW). The difference in the light and heavy hole

masses results in a splitting of the miniband spectrum in the valence band that can (in the case of deep and narrow quantum wells for holes) exceed the splitting in a stressed GaAs layer. The main advantage of SL-based photoemitters is the possibility to vary the properties of the active layer over a wide range by the appropriate choice of layer composition, thickness, and doping [7-9].

Below we report results on polarized electron emission from a new strained short-period AlInGaAs-GaAs superlattice with a minimal conduction-band offset. We show that the performance of this new superlattice exceeds that of the GaAs strained layer cathodes and the potential for further improvements is favourable.

Description of samples. In SL-based cathodes the thickness of the active layer is restricted mainly by the spin diffusion length. In previously used $Al_xGa_{1-x}As/GaAs$, $In_xGa_{1-x}As/GaAs$ [6,9] and $Al_xGa_{1-x}As/In_yGa_{1-y}As$ SL [6,9,10], the hole miniband splitting was accompanied by the building of high barriers for electrons as a result of the high value of the ratio of the conduction-band offset ΔE_c to the valence-band offset ΔE_v ($\Delta E_c/\Delta E_v \approx 2$) at the heterointerface. The necessity for the electrons to tunnel through the SL barriers results in a lower electron diffusion rate along the SL axis accompanied by growth of the spin relaxation rate [11,12]. This leads to electron depolarization during their diffusion to the surface.

The main advantage of the $Al_xIn_yGa_{1-x-y}As/GaAs$ SL proposed here comes from the band line-up between the semiconductor layers of the SL. The Al content determines the formation of a barrier in the conduction band, while adding In leads to conduction band lowering, so the conduction band offset can be completely compensated by appropriate choice of x and y, while barriers for the holes remain uncompensated. Therefore the use of superlattices with the optimized quaternary alloy composition can provide a high vertical electron mobility and simultaneously a small spin relaxation rate while also maintaining a sufficiently large valence-band splitting.

The SL samples were grown by solid-source molecular beam epitaxy in a Riber32P machine on GaAs(100)-oriented substrates. The native oxide layer was removed from the top of the substrate at 630°C in the growth chamber under an As flux. Then 0.2μm-thick GaAs: Be ($4\times10^{18}cm^{-3}$) and 0.4μm-thick $Al_{0.3}Ga_{0.7}As$: Be ($4\times10^{17}cm^{-3}$) layers were deposited at 600°C. Growth was interrupted, and the substrate temperature was decreased to 510°C to prevent In re-evaporation and Be segregation effects in the active SL.

The SL samples consisted of 17 (or 15) pairs of GaAs(4nm) and AlInGaAs(4nm) doped with Be and were terminated by a 6nm (or 8nm) heavily-doped GaAs layer capped with As to ensure stable activation and an NEA surface state. The parameters of the samples are listed in Table 1. The procedure of mole fraction and layer thickness estimation was based on knowledge of growth rates of AlAs and InAs binary compounds.

Table 1. The strained $Al_xIn_yGa_{1-x-y}As$/GaAs superlattice samples.

Sample	1 (2-943)	2 (3-171)	3 (3-335)	4 (3-336)
Be doping	3×10^{18a}	5×10^{17b}	4×10^{17b}	4×10^{17b}
d, mkm	0.12	0.136	0.136	0.136
x, %	18	18	18	20
y, %	18	16	18	18
E_{ex}, eV	1.39	1.435	1.42	1.45
Pol.(max), %	79.5	73.3	79.1	86 (82.7)
Y(pol.max), %	7.4×10^{-3}	6×10^{-2}	7×10^{-3}	7.5×10^{-3} (9.4×10^{-2})

[a] Homogeneous doping including the last GaAs layer

[b] Modulation doping, the last GaAs layer is heavily doped, $p\geq4\times10^{18}$ cm^{-3}

The GaAs growth rate was determined from the quantum-well width-dependent photoluminescence (PL) peak position of an AlAs/GaAs QW structure. The InAs growth rate was determined from the onset of the island growth mode when an InAs film is deposited on a GaAs substrate. This transition takes place at 1.7 monolayer of InAs. All these layers, which are necessary for growth rate estimation, were grown on one test sample and quickly measured by PL. The relationship between the AlAs mole fraction in the AlGaAs layer and the PL peak position as well as the dependence of the QW PL peak position on the QW width have been previously determined by comparison of the PL, X-ray diffraction data, and in situ growth rate measurements using the RHEED oscillation technique.

All the samples were capped by As using the following procedure. Just after the deposition of the last layer of the structure, the substrate heater was switched off and then the sample was cooled down in the growth chamber for one hour. The sample was turned to face a liquid nitrogen cryoshroud. At the end of this stage the substrate temperature was usually around 30°C. Then the sample was placed again in the growth position opposite the As source for 1.5 hour. At the end of this second stage the substrate temperature was around 0°C. The As cap thickness was estimated to be 0.1mm based on Auger profiling measurements.

The characterization of the samples was done using luminescence and X-ray diffraction techniques. The X-ray diffraction patterns show that in the case of the GaAs substrate and $x\leq0.2$, the strain relaxation in the thin 4-nm $Al_xIn_yGa_{1-x-y}As$ layers remains negligible for the total SL thickness, d, up to $d\cong150$ nm.

Choice of the SL layer composition. The miniband spectrum of the SL is determined by the band offsets at the heterointerfaces. In the case of a heterointerface with lattice matched ternary solid solution (e.g. $Al_xGa_{1-x}As$-GaAs) the conduction-band offset ratio, Q_{c1}, is defined as $Q_{c1}=\Delta E_c(x)/\Delta E_{g1}(x)$, where $\Delta E_{g1}(x)$ is the difference in the band gaps of the contacting crystals so that the valence band offset ratio, Q_v, is $Q_v=1-Q_c$. For an $In_yGa_{1-y}As$-GaAs interface the offset is modified by the strain distribution in the contacting layers. For the structure with a thin $In_yGa_{1-y}As$

layer grown on a thick GaAs substrate all the strain is assumed to accumulate in the InGaAs layer. For this case $\Delta E_c(y)=Q_{c2,def}\times(\Delta E_{g2}(y)+\delta E_{g2}^{def}(y))$. Here $Q_{c2,\,def}$ is the conduction band offset ratio for the strained $In_yGa_{1-y}As$ layer while, $\delta E_{g2}^{def}(y)$ is the change of the band gap induced by strain that can be expressed through interpolated deformation potentials, elastic constants, and the lattice constant mismatch (see e.g. ref. [13,14]). The other way to calculate the offset (which should give the same result [14]) is to use the offset ratio for unstrained layers, Q_{c2}, and then include the strain effects, so that $\Delta E_c(y)=Q_{c2}\times\Delta E_{g2}(y)+\delta E_{g2}^{def}(y)$. For the case of the $Al_xIn_yGa_{1-x-y}As$/ GaAs SL, a linear interpolation between the values for $Al_xGa_{1-x}As$-GaAs and $In_yGa_{1-y}As$-GaAs interfaces should be valid for small x and y. We have found that interpolation starting with the unstrained value of the band offset for the $In_yGa_{1-y}As$-GaAs heterointerface gives band-gap values that are far from the experimental data obtained from emission spectra. Using the band offset value for the strained $In_yGa_{1-y}As$-GaAs interface, we get:

$$\Delta E_c(x,y)=Q_{c1}\times\Delta E_{g1}(x)+Q_{c2,\,def}\times(\Delta E_{g2}(y)+\delta E_{g2}^{def}(y)$$

The schematic of the position of the band edges for x=0.20, y=0.18 is shown in Fig.1. Taking Q_{c1}=0.66 [15] and $Q_{c2,\,def}$=0.7 [14] we have found that the conduction band offset appears to be minimized for x=1.1y.

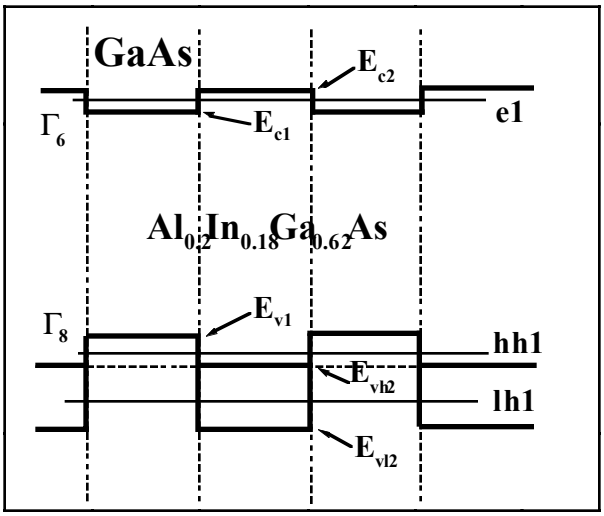

Fig.1. Energy band diagram of $Al_xIn_yGa_{1-x-y}As$/GaAs SL. The minibands (thin lines) are identified by notation e1 and hh1, lh1 for electrons and holes respectively.

Another (more consistent) approach for the quaternary alloys starts with calculating the band gap of the alloy and the absolute average valence band position in the alloy [13]. Then the deformation shifts of all the bands are calculated using an interpolation for the deformation potentials and elastic constants with a set of bowing

coefficients to account for nonlinear terms. We have found that both approaches give close numerical results that do not exactly fit our experimental data, which can be attributed to the uncertainty of the bowing coefficients and also to the partial strain relaxation and some tensile deformation of the GaAs layer (see below). The calculated positions of the band edges (following the approach of ref. [13]) of the layers in the strained SL samples are given in Table 2. It is seen that for all samples calculated values of the conduction band offset does not exceed 20meV. For the thermalized electrons at room temperature the influence of the resulting periodical potential should be negligible. Besides, as a result of the conduction-band line up, the 4-nm barriers for the electrons in the SL are transparent. Thus the changes of electron mobility and spin relaxation rate should be small compared to pure GaAs.

Table 2. The positions (in electron volts) of the band edges in $Al_xIn_yGa_{1-x-y}As$/GaAs SL samples.

Sample	E_{vh2}[a]	E_{vl2}	E_{c1}[a]	E_{c2}	E_{g1}	E_{g2}
2[b]	-0.051[c]	-0.124	1.423	1.442	1.422	1.492
3[b]	-0.043	-0.126	1.423	1.429	1.421	1.472
4[b]	-0.056	-0.138	1.423	1.445	1.422	1.501

[a] 1- GaAs, 2- $Al_xIn_yGa_{1-x-y}As$ layer.

[b] Composition of the layers is given in Table 1.

[c] Zero energy is at valence band of the GaAs layer.

It is seen from Fig.1 and the data of Table 2 that the strain of the $Al_xIn_yGa_{1-x-y}As$ layers produces barriers for both heavy and light holes, the barrier for the light holes being 75meV higher, which leads to additional hole-miniband splitting favourable for the electron optical orientation.

The choice of the layer thickness is dictated by the need to split the hole minibands. The splitting grows when barriers are broad enough and wells are narrow and deep. Still the thickness of the strained $Al_xIn_yGa_{1-x-y}As$ layer should be less than the critical thickness $h_c(y)$. The overall critical thickness for the superlattice with alternating layers of equal thickness can be estimated as $H_c=h_c(y/2)$. The thickness of a single $Al_xIn_yGa_{1-x-y}As$ layer was taken to be 4nm (to be less than the calculated $h_c(y)$), and in accordance with X-ray data the chosen thickness of the SL samples (d=0.12-0.136μm) exceeded H_c much less than in the case of a cathode structure with one strained GaAs layer.

Experimental results. The Mott analysers both at St. Petersburg Technical University (SPTU) [16] and at the Stanford Linear Accelerator Center (SLAC) [17] were used to measure the spin polarization of photoelectrons.

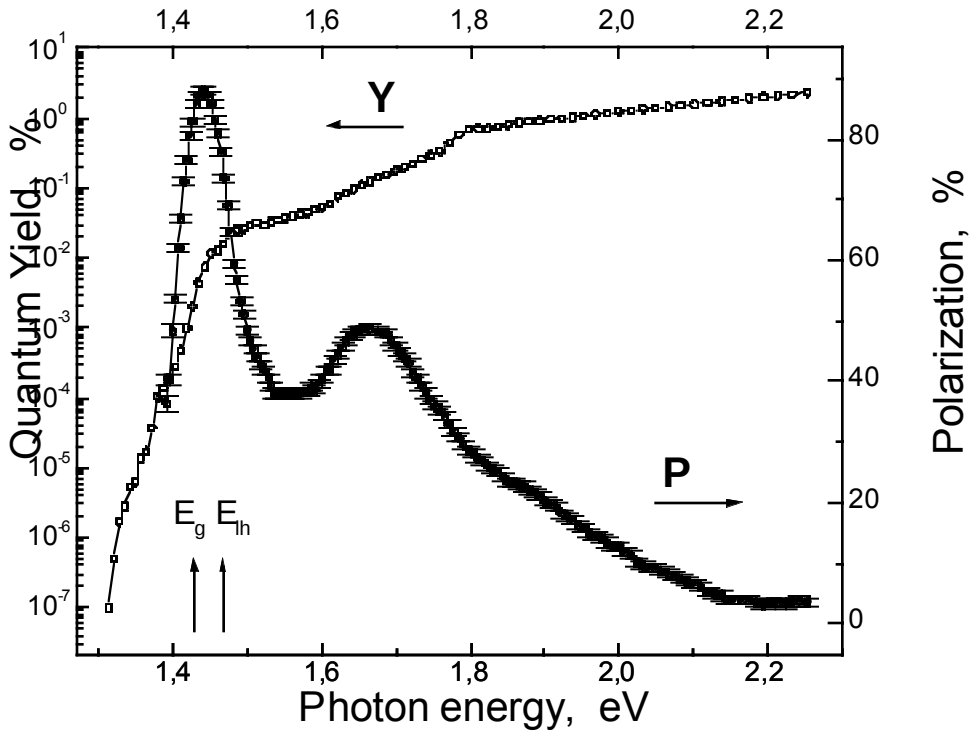

Fig.2. Electron spin polarization and quantum yield as a function of excitation energy for sample 4 (SPTU data). The band gap energy E_g and the light hole excitation energy E_{lh} are indicated by arrows.

In Fig.2 the polarized emission and quantum yield data measured at SPTU are shown as a function of the optical excitation energy for the 3-336 SL (sample 4). The maximum polarization obtained with local optical excitation was 86% and the corresponding quantum yield, Y, was 7.5×10^{-3}%. Y for the excitation energy, E_{ex}, at the polarization maximum is sensitive to activation procedure and vacuum in the setup. At SLAC, P=82.7% with Y=9.4×10^{-2}% was obtained. In Fig.3 polarization and quantum yield spectra for the sample 3 obtained at SLAC and at SPTU are presented. Sample 3 was chosen to compare data since the time lapse between the two data sets for sample 3 was very short. We have found the polarization results to be similar despite the somewhat different techniques of sample preparation, activation, and vacuum. Due to better vacuum conditions in the SLAC apparatus, the values of quantum yield measured at SLAC were regularly higher than those measured at SPTU.

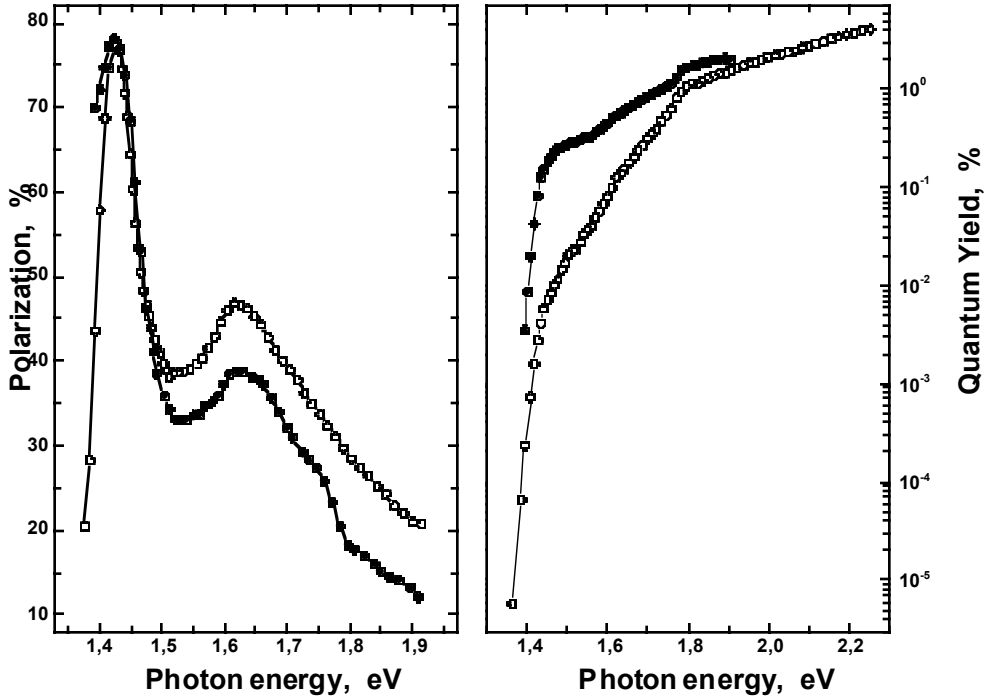

Fig.3. Polarization and quantum yield spectra for the sample 3: SPTU measurements - open circles, SLAC - full circles.

The observed emission spectra can be interpreted in terms of a three-step model linearized for the thin-film emitter case [8]. The linearized Y is given by:

$$Y = (1-R)\frac{\tau_1}{\tau_1+\tau_{emi}}\alpha d \,, \qquad (1)$$

where α is the optical absorption and R is the reflection coefficient, τ_1 is the electron lifetime in the band bending potential well, τ_{emi} is the time of electron emission in vacuum. According to Eq.(1), Y(hv) reproduces the optical absorption spectrum. The emitted electron polarization can be expressed as

$$P = P_0(1-d/(S_0\tau_S))\frac{\tau_{S1}}{\tau_{S1}+\tau_{emi}}, \qquad (2)$$

where P_0 is the initial electron polarization upon excitation by circularly polarized light, S_0 is the surface recombination velocity, τ_S is the spin relaxation time in the SL, τ_{S1} the spin relaxation time in the band bending region. The factors in Eq.(2) account for polarization losses at three steps of emission process. The polarization dependence on the excitation energy comes from P_0 and also the electron escape time d/S_0 into the band bending region. The decrease of the polarization from its maximum value with decreasing excitation wavelength starts with electron excitation from the first light-hole miniband. The falloff of polarization as excitation drops below the conduction band minimum can be associated with electron excitation in the tail states

of potential wells which increases the electron escape time. A sharp decrease of Y and P below the band edge indicates a small tail size for the chosen doping level.

Thus, the position of the polarization maximum is close to the SL band gap. In the SL the band gap is larger than that in GaAs layers by quantization energy of the heavy holes and some shift of the conduction band minimum. Calculation of the miniband energies using the model described in [18] gives absolute values of the hole miniband energies E_{hh1}=13meV, E_{lh1}=54meV, the difference of these values for small changes of the layer composition is within the errors of determination of the band edges. The edge of the electronic band in a SL with a small conduction-band offset is close to the average conduction-band energy in the contacting layers.

The calculation of the band gap using the data given in Table 2 in $E_g=E_{g1}+E_{hh1}+((E_{c2}-E_{c1})/2)$ gives for all samples values that exceed the experimentally observed energy of the polarization maximum by ~20 meV. This shift of the band gap values is equivalent to additional ≈3% of Al concentration. The regular difference in the calculated and observed band gap value in the strained quaternary alloy can be attributed to the uncertainties in the conduction band offset calculations and also to some tensile deformation of GaAs layer resulting in less strain in the contacting $Al_xIn_yGa_{1-x-y}As$ layer.

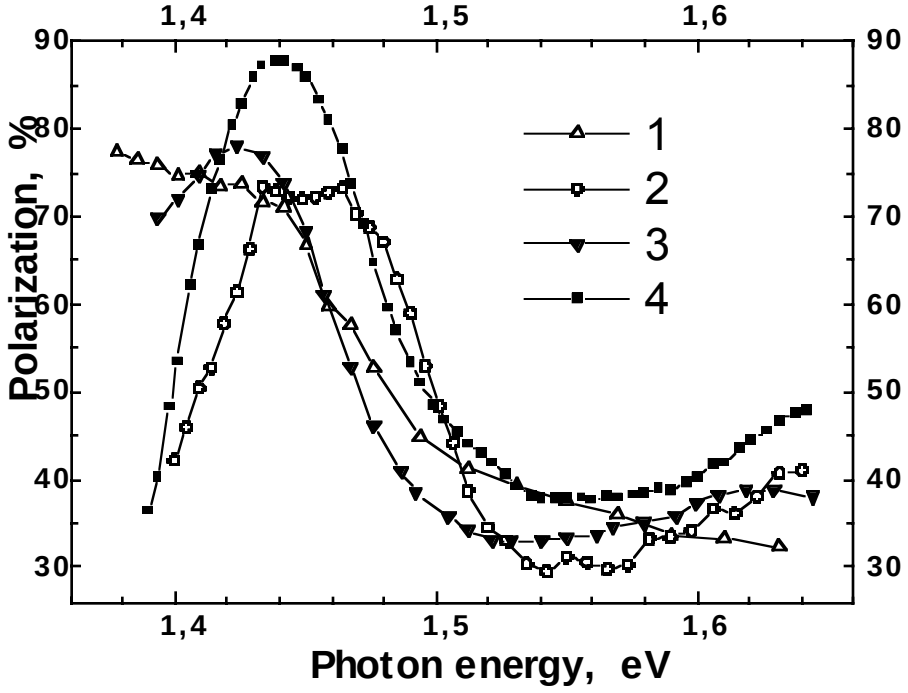

Fig.4. The electron spin-polarization spectra near the excitation edge for the superlattice samples with different layer composition. The samples: 1- up-triangles, 2-circles, 3 - full down-triangles, 4-full boxes.

This misfit can be rather easily corrected by choosing a SL with larger x when some tuning of the SL band gap to excitation source is needed. Indeed, adding of Al does not influence the deformation so that the band gap variation with x is predictable.

In Fig.4 the measured polarization of the emitted electrons for all the samples in the vicinity of the absorption edge is presented. The absolute value of maximum shift is consistent with the expected change on the basis of the data in Table 2. The width of the polarization maximum is consistent with a splitting of ≈40meV between the hh1 and lh1 minibands. One can expect larger splittings with thicker barriers and thinner GaAs wells. Then, one can expect a smaller spin relaxation rate for optimally chosen doping of the SL, compatible with needed extracted emission current.

Thus, the optimization of the SL structure parameters and doping profile can lead to further improvement of the proposed new SL photoemitter structure.

Finally, the maximum current density that can be extracted from these SL samples at high voltage has yet to be determined. Initial measurements using samples 2 and 3 gave anomalously low values. Definitive measurements are underway.

Conclusions

In conclusion, electron spin polarization as high as 86% has been reproducibly obtained from strained $Al_xIn_yGa_{1-x-y}As/GaAs$ superlattice with minimal conduction band offset at the heterointerfaces. The modulation doping of the SL provides high polarization and high quantum yield at the polarization maximum. The position of the maximum can be easily tuned to an excitation wavelength by choice of the SL composition. Further improvement of the emitter parameters can be expected with additional optimization of the SL structure parameters.

Acknowledgements

This work is supported by the U.S. Civilian Research and Development Foundation under Award No. RP1-351. Support of Russian State Program "Surface atomic structures", project No. 95-1.23 and Russian Foundation for Basic Research, project No. 96-02-19187 is also gratefully acknowledged.

REFERENCES

[1] T.Maruyama et al., Phys. Rev. Lett., **66,** (1991), 2376; T.Nakanishi et al., Phys. Lett. A **158**, (1991), 345.

[2] D.T.Pierce in Atomic, Molecular, and Optical Physics: Charged Particles, F.B.Dunning and R.G.Hulet eds., San Diego: Academic Press (1995), 1.

[3] J.E.Clendenin, Int. J. Mod. Phys. A **13**, (1998), 2507.

[4] F.Ciccacci et al., Rev. Sci. Instrum, **68**, (1997), 1841.

[5] H.Tang et. al. in Proc. of the 4th European Particle Accelerator Conf., May 17-23, 1994, London, UK (World Scientific, Singapore, 1994), 46.

[6] K.Togawa et al., Nucl. Instrum. and Meth. A **414**, (1998), 431.

[7] A.V.Subashiev, in Proc. Intern. Semicond. Device Research Symposium, Charlottesville, USA, 1995, (Academic Outreach, School of Engineering and Applied Science, Charlottesville, USA), **1**, 217.

[8] A.V.Subashiev, in Proc. 12-th Intern. Symp. On High-Energy Spin Physics, Amstardam, 1996, ed. by C.D.W. de Jager et al. Word Scientific, Singapore, (1997), 749.
[9] T.Nakanishi et al., in .Proc. 7-th Intern. Workshop On Polarized Gas Targets and Polerized Beams, Urbana, 1997, ed. by R.J.Holt and M.A.Miller, AIP Conf. Proc. 421, 300.
[10] Yu.Mamaev et al., Phys. Low-Dim. Structures, **10/11**, (1995), 61.
[11] M.J.Snelling et al., J. Luminescense, **45**, (1990), 208.
[12] P.Baumgart et al., Appl.Phys.Lett., **64**(5), (1994), 592.
[13]M. C.P.Krijn, Semicond. Sci. Technol. **6**, (1991), 27.
[14] D.J.Arent et al., Appl.Phys. **66**, 940, 1739, (1998)
[15] G.Ji.Huang et al., J. Vac. Sci. Technol. **B5**, (1998), 1346.
[16] Yu. Yashin et al., this volume
[17] G.Mulhollan in Proc. of the Workshop on Photocathodes for Polarized Electron Sources for Accelerators, SLAC-432, (1994), 211.
[18] L.G.Gerchikov, G.V.Rozhnov, A.V.Subashiev, Sov. Phys. JETP, **74**, (1992), 77.